Segmentation of Benign and Malign lesions on skin images using U-Net

Elif Işılay ÜNLÜ
Computer Engineering
Firat University
Elazığ, TURKEY
eiunlu@firat.edu.tr

Ahmet ÇINAR
Computer Engineering
Firat University
Elazığ, TURKEY
acinar@firat.edu.tr

2021 International Conference on Innovation and Intelligence for Informatics, Computing, and Technologies (3ICT) | 978-1-6654-4032-5/21/$31.00 ©2021 IEEE | DOI: 10.1109/3ICT53449.2021.9581463

***Abstract*— One of the types of cancer that requires early diagnosis is skin cancer. Melanoma is a deadly type of skin cancer. Computer-aided systems can detect the findings in medical examinations that human perception cannot recognize, and these findings can help the clinicans to make an early diagnosis. Therefore, the need for computer aided systems has increased.**

In this study, a deep learning-based method that segments melanoma with color images taken from dermoscopy devices is proposed. For this method, ISIC 2017 (International Skin Image Collaboration) database is used. It contains 1403 training and 597 test data. The method is based on preprocessing and U-Net architecture. Gaussian and Difference of Gaussian (DoG) filters are used in the preprocessing stage. It is aimed to make skin images more convenient before U-Net. As a result of the segmentation performed with these data, the education success rate reached 96-95%. A high similarity coefficient obtained. On the other hand, as a result of the training of the preprocessed data, accuracy rate has reached 86-85%.

Keywords—Deep learning, image segmentation, melanoma, U-Net

I. INTRODUCTION

Skin cancer is one of the most important diseases in dermatology. Skin cancer is a type of cancer that can be lethal, therefore it's critical to get a diagnosis as soon as possible. An estimated 106,110 adults (62,260 men and 43,850 women) will be diagnosed with invasive melanoma of the skin this year in the United States[1].

In recent years, image processing techniques have played an important role in analyzing medical images in a wide variety of ways. Image processing techniques are indispensable to reduce the noise and blur of the medical image. In addition to image processing techniques, the use of deep learning methods has brought advantages in terms of both accuracy and speed.

Deep learning is the general name given to machine learning algorithms used to create systems that think and make decisions like humans. Deep learning aims to perform learning and decision-making processes by modeling a structure similar to the human brain [2]. Deep learning methods are widely used in the medical field for tasks such as image classification, object detection, and segmentation[3].

Segmentation is usually the first step of image analysis. Image segmentation can be described as dividing an image into meaningful regions in which different features are retained. There are basically two different segmentation techniques. These are Semantic Segmentation and Instance Segmatation.

Many deep learning models have been used in image segmentation studies. Some of those; FCN(Fully Convolutional Networks), SegNet, RefineNet, U-Net, DeepLab, R-CNN etc. [4]. Studies on segmentation in the literature have generally focused on brain MR images.

Akkuş et al evaluated various CNN architectures and performance measures for the brain segmentation task on MR images [5].

Moeskops et al used 3 CNNs with different two-dimensional input channels to classify and segment different tissues from MRI images of 35 adult and 22 premature infant subjects. With the method they used, they obtained dice coefficients of 0.87, 0.82, 0.84, 0.86 and 0.91 on all segmented tissue classes, respectively, for each data set [6].

Preira et al. used deeper CNN architectures consisting of 11 layers. They used small 3x3 filters to avoid problems such as Overfitting, which are common in deeper networks. Their method was validated in the Brain Tumor Segmentation Competition 2013 database (BRATS 2013), and they obtained Dice similarity coefficients of 0.88, 0.83, 0.77 for whole, core, and enhancer regions. Using the same model, they came second in the BRATS 2015 competition and obtained Dice similarity coefficients of 0.78, 0.65 and 0.75 [7].

In a study by Li and Shen in 2017, two different deep learning methods were proposed for tasks such as lesion segmentation, feature extraction and lesion classification. These methods have been tested on the ISIC 2017 dataset. Accuracy values of 0.753, 0.848 and 0.912 were obtained for different tasks [8].

Yuan, Chao and Lo used deep convolution-deconvolutional neural networks (CDNN) for segmentation of skin lesions on dermoscopic images. And they obtained an average Jaccard index of 0.784 in the dataset [9].

Xu and Hwang performed automated skin lesion analysis with the ISIC 2018 dataset and the U-Net model. They tested 5 models with 100 validation images and obtained a segmentation score of over 0.70 for each model [10].

Tang et. al. proposed a U-net based skin lesion segmentation method. Experimental results showed that the proposed approach segmented skin lesions with the International Skin Imaging Collaboration (ISIC) 2016 Skin Lesion Difficulty (SLC) data set, the average Dice coefficient 93.03% and Jaccard index 89.25% for 86.93% and 79.26%. 94.13% and 89.40% for ISIC 2017 SLC and PH2 dataset, respectively [11].

In the second section, the data set used for the developed method, pretreatment stages are mentioned, the architecture used in the segmentation stage of the skin images with a deep learning based system is explained and interpreted together with the application results.

In the last section, the results obtained and the studies planned for the future are mentioned.

II. MATERIAL AND METHOD

A. Dataset

In this study, the publicly available ISIC (International Skin Imaging Collaboration) archive was used as a data set [12]. A total of 2000 color skin images were used. 1403 of them were taken as training data and 597 as test data. In the training dataset, there are 1403 images of 128x128 skin lesions in jpeg format and 1403 ground truth segmentation images in png format. Some examples of original images are as in Fig 1.

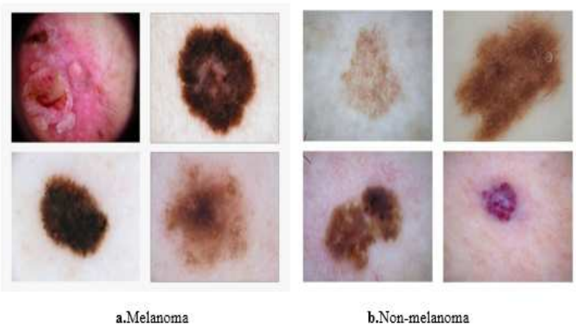

Fig. 1. a.Diseased images , b.Healthy images [12]

B. Preprocessing

Gaussian and Difference of Gaussian (DoG) filters are applied to the images in the preprocessing step. The Gaussian filter is a 2D convolution operator used to blur images and remove noise. It is used to apply a smoothing operation on a given image. In other words, it removes the noise on the image. The formula of the Gaussian filter is as in (1). Here σ is the standard deviation of the distribution.

$$G(x) = \frac{1}{\sqrt{2\pi\sigma}} e^{-\frac{x^2}{2\sigma}} \tag{1}$$

Difference of Gaussian (DoG) The difference of the Gaussian module is a filter that defines edges. DoG performs edge detection by performing Gaussian blur on a specified image [13][14]. The DoG as an operator or convolution kernel is defined as (2):

$$DoG \triangleq G_{\sigma_1} - G_{\sigma_2} = \frac{1}{\sqrt{2\pi}} \left(\frac{1}{\sigma_1} e^{-(x^2+y^2)/2\sigma_1^2} - \frac{1}{\sigma_2} e^{-(x^2+y^2)/2\sigma_2^2} \right) \tag{2}$$

The original and filtered samples of the images are as in Fig. 2.

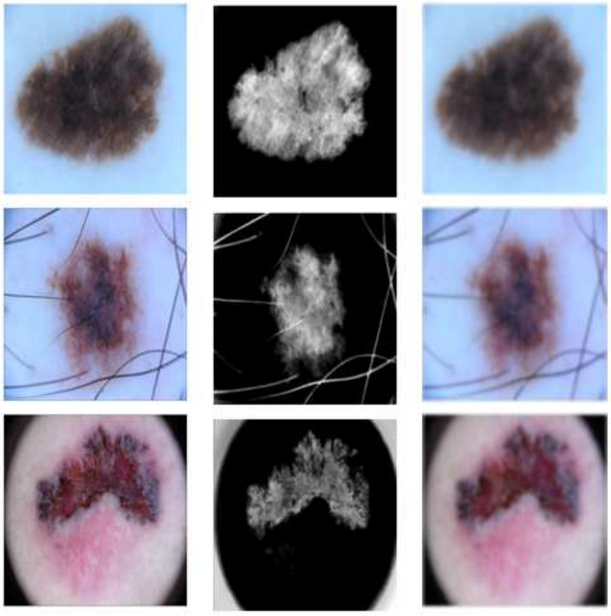

Fig.2. Training dataset images a. Original images b. Images with the Difference of Gaussian(DoG) applied c. Images with the Gaussian applied.

C. Developed Model

In the developed system, the data is trained using U-Net, one of the deep learning models. It has a "U" shape. U-Net architecture is symmetrical and its operation is somewhat similar to autoencoders. It can be narrowed down into three main parts - the Narrowing (downsampling) path, the Bottleneck, and the expanding (upsampling) path. The downsampling path is a typical convolutional network. It consists of 4 blocks and each block contains 2 3x3 convolution layers + activation functions (with batch normalization) and one 2x2 maximum pooling layer. In autoencoders, the encoder part of the neural network compresses the input into a hidden field representation, and then a decoder generates the output from the compressed or encoded representation. But there is a slight difference, unlike normal encoder-decoder structures, the two parts are not decoupled. Skip connections are used to transfer fine-grained information from the lower-level layers of the analysis path to the higher-level layers of the synthesis path, as this information is needed to create accurate fine-grained reconstructions[15]. The network architecture is shown in Fig. 3. An overview of the proposed method is as in Fig 4.

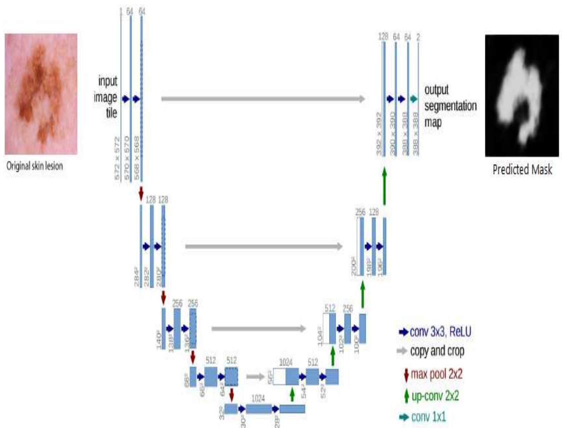

Fig. 3. U-Net Model

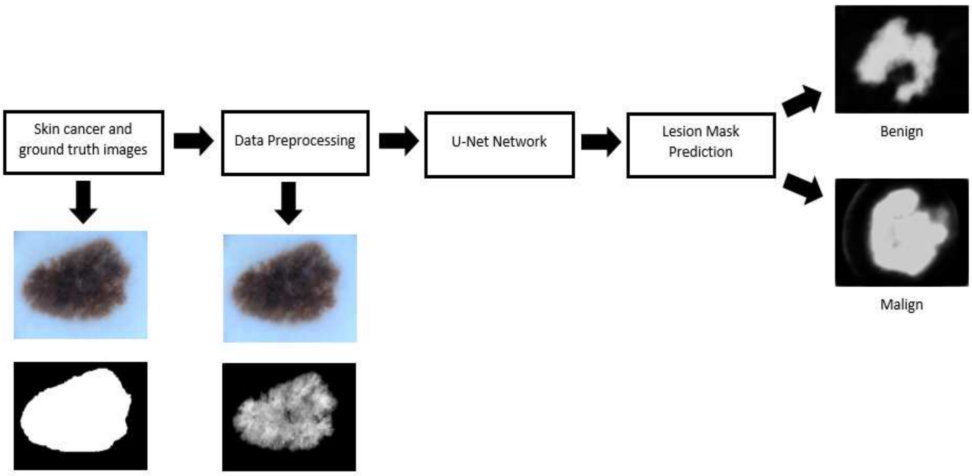

Fig 4. General view of proposed method

In our proposed method, lesion segmentation is performed from skin images using U-Net convolutional neural network. Raw skin images, preprocessing skin images and ground truth masks are trained with the U-Net network for the lesion segmentation process. As a result of the training, segmentation masks of the test images labeled as malignant and benign are obtained.

III. RESULTS AND DISCUSSION

Original skin images and preprocessed images are trained individually in 100 epochs with the U-Net model. Sgd is used as the optimization method and sigmoid was used as the activation function. The binary mask images obtained from expert dermatologist is provided as ground truth files. As test data, 493 skin images were given and predictive masks were produced. Raw images and preprocessed images, ground truth images and predicted binary masks are shown in Fig. 5. The accuracy and error values after the training are as in Fig. 6, Fig. 7 and Fig. 8. After training the original images and Gaussian filtered images, the accuracy rate reached 95%, while the accuracy rate of DoG(Difference of Gaussian) filtered images is about 85%.

When the results of the predictions are examined visually, the results are quite similar to the actual segmentation results. In the results of the preprocessing, it was observed that the area surrounding the lesion was more soft segmented. In other words, thin boundaries were lost in the segmentation results. Predicted binary mask results obtained after preprocessing are not satisfactory.

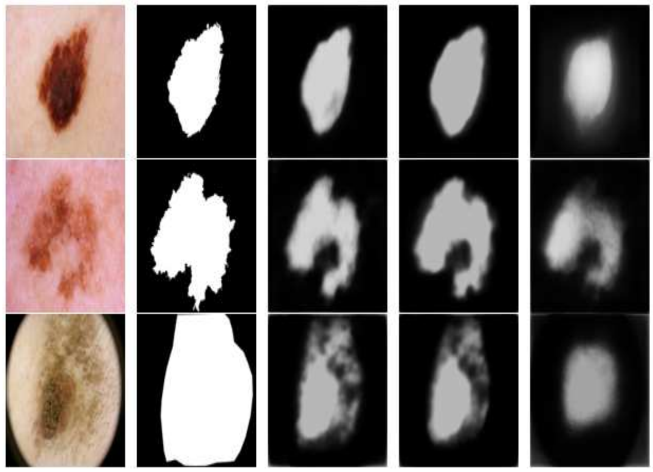

Fig.5. Test images and prediction results a. Original skin images b.Ground truth images c.Predicted masks of original images d. Predicted masks image of Gaussian filter e.Predicted masks image of DoG filter

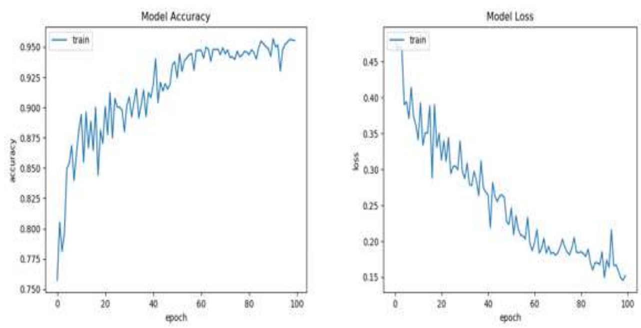

Fig. 6. Accuracy (Left) and Loss (Right) Rates in 100 Epoch

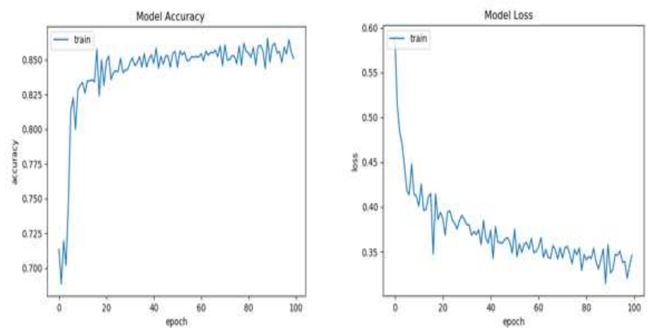

Fig. 7.Accuracy (Left) and Lost (Right) Rates of DoG filter images in 100 Epoch

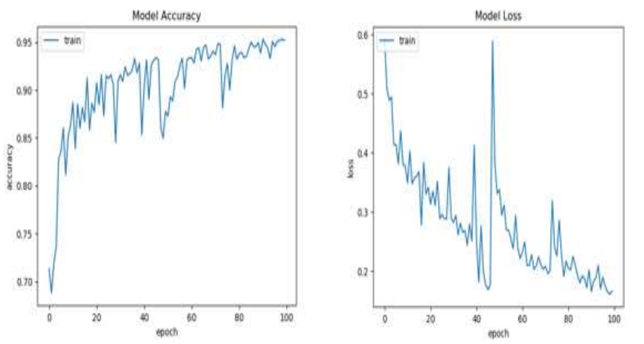

Fig. 8. Accuracy (Left) and Lost (Right) Rates of Gaussian filter images in 100 Epoch

Some studies used in the segmentation of melanoma are examined in Table 1. These studies have shown that FCN and UNet architectures give successful results in medical image segmentation. In our proposed method, we obtained a higher accuracy rate by using less data compared to other studies. Unlike other studies the foreign objects such as hair, ruler marks, etc. are not removed from the images in the preprocessing step.

TABLE 1. STUDIES ON SKIN LESION SEGMENTATION

References	Method	Acc.	Dice	Jacc.	Dataset
Akkuş et al.	CNN	0.88	-	-	Brain MRI images
Moeskop et al.	CNN	-	0.87 0,82 0,84 0,86 - 0,91	- -	Tissue MRI images
Preira et. al.	CNN	- -	0,88- 0,83 -0,77 0,78 – 0,65-0,75	-	BRAST 2013 BRAST 2015
Li and Shen	FCRN	0,753 0,848 0,912	- - -	- - -	ISIC 2017
Yuan et. al.	CDNN	-	-	0,784	ISIC
Xu and Hwang	U-Net	0,749	-	-	ISIC 2018
Tang et. al.	U-Net	- - -	0,93 0,86 0,94	0.89 0.79 0.89	ISIC 2016 ISIC 2017 PH2
Proposed Method	U-Net	0,95 0,85	- -	- -	ISIC 2017

CONCLUSION

Automated analysis of dermoscopic images can help dermatologists in clinical decision making and even help patients evaluate skin lesions outside the hospital. To perform automated analysis of dermoscopic images, the separation of skin lesions from the normal region is usually the first step. In this study, a method with a deep network architecture has been proposed to determine the lesion site from skin images. U-Net architecture is used for lesion determination. As a result of the training of the original images and gaussian filter images, the accuracy rate reached to 95% and the accuracy rate of the DoG(Difference of Gaussian) filter images reached 85%.Segmentation of raw images gave similar or even better results to ground truth images. As a result of segmentation of pre-processed images, the lesion boundaries were not clearly determined.

The results of this study show that deep learning constructs have a significant impact on the diagnosis of melanoma. It is think that the performance of the system will increase by expanding the used data set and trying different segmentation methods.

AUTHORS AND AFFILIATIONS

All authors contributed equally to the study.

Elif Işılay ÜNLÜ, Fırat University., departman of Computer Engineering Elazığ, Türkiye*
Ahmet ÇINAR, Fırat University., departman of Computer Engineering, Elazığ, Türkiye
*Corresponding author: eiunlu@firat.edu.tr

Statement of Research and Publication Ethics
The author declares that this study complies with Research and Publication Ethics

REFERENCES

[1] Melanoma: Statistics , https://www.cancer.net/cancer-types/melanoma/statistics

[2] L. Deng,, and Y. Dong,,. Deep Learning Methods and Applications, 198-349, 2014.

[3] S. Jayasumana ,Semantic Image Segmentation with Deep Learning,2015.

[4] A 2017 Guide to Semantic Segmentation with Deep Learning ,Sasank Chilamkurthy, [online]24.03.2019.
http://blog.qure.ai/notes/semantic-segmentation-deep-learning-review

[5] Z. Akkus, A. Galimzianova, A. Hoogi, D. L. Rubin, and B. J. Erickson, ``Deep learning for brain MRI segmentation: State of the art and future directions,'' J. Digit. Imag., vol. 30, no. 4, pp. 449-459, 2017.

[6] P. Moeskops, M. A. Viergever, A. M. Mendrik, L. S. de Vries, M. J. N. L. Benders, and I. Isgum, ``Automatic segmentation of MR brain images with a convolutional neural network,'' IEEE Trans. Med. Imag., vol. 35, no. 5, pp. 1252-1261, May 2016.

[7] S. Pereira, A. Pinto, V. Alves, and C. A. Silva, ``Brain tumor segmentation using convolutional neural networks in MRI images,'' IEEE Trans. Med. Imag., vol. 35, no. 5, pp. 1240-1251, May 2016.

[8] Y. Li ,L. Shen "Skin Lesion Analysis towards Melanoma Detection Using Deep Learning Network", Sensors, Feb 2018.

[9] Yading Yuan, Ming Chao and Yeh-Chi Lo, "Automatic skin lesion segmentation with fully convolutional-deconvolutional Networks" IEEE Journal of Biomedical and Health Informatics, 2018.

[10] H. Xu Tae ,H. Hwang, "Automatic Skin Lesion Segmentation Using Deep Fully Convolutional Networks",2018

[11] Peng Tang , Qiaokang Liang , Xintong Yan , Shao Xiang , Wei Sun , Dan Zhang , Gianmarc Coppola "Efficient skin lesion segmentation using separable-Unet with stochastic weight averaging" ELSEIVER Computer Methods and Programs in Biomedicine, 178, 289–301,2019.

[12] International Skin Imaging Collaboration,https://www.isic-archive.com

[13] https://homepages.inf.ed.ac.uk/rbf/HIPR2/hipr_top.htm

[14] http://fourier.eng.hmc.edu/e161/lectures/gradient/node9.html

[15] O. Ronneberger, P. Fischer, and T. Brox "U-Net: Convolutional Networks for Biomedical Image Segmentation", , Medical Image Computing and Computer-Assisted Intervention (MICCAI), Springer, LNCS, Vol.9351: 234--241, 2015.

[16] R. Lopez, X Giró-i-Nieto,A. Marques Skin Lesion Detection from Dermoscopic Images using Convolutional Neural Networks. O. 2017.

[17] E.I., Ünlü, and A. Çınar, Classification of Skin Images with Respect to Melanoma and Non-Melanoma Using the Deep Neural Network, IOSR Journal of Engineering (IOSRJEN), 8(12), pp. 35-40. 2018.

[18] Y. Bengio,., P. Lamblin, D. Popovici, and H. Larochelle,, Greedy Layer-Wise Training of Deep Networks, Advances in Neural Information Processing Systems. 2007.

[19] A. Karpathy, Convolutional Neural Networks (CNNs / ConvNets). Retrieved CS231n Convolutional Neural Networks for Visual Recognition. 2016.

[20] Lo, S., Lou, C., Lin, S.L., Freedman, J.S., Chien, M.T., M.V., and Mun, S.K., 1995. Artificial convolution neural network techniques and applications for lung nodule detection. IEEE Transactions on Medical Imaging, 14(4), 711-718.